HHS Public Access

Author manuscript

Nature. Author manuscript; available in PMC 2012 February 23.

Published in final edited form as:

Nature. 2011 February 24; 470(7335): 535–539. doi:10.1038/nature09742.

Synaptic potentiation onto habenula neurons in learned helplessness model of depression

Bo Li[1,2,*,#], **Joaquin Piriz**[1,*], **Martine Mirrione**[2,3,*], **ChiHye Chung**[1,*], **Christophe D. Proulx**[1], **Daniela Schulz**[3], **Fritz Henn**[2,3], and **Roberto Malinow**[1,#]

[1]Center for Neural Circuits and Behavior, Departments of Neuroscience and Biological Sciences, University of California at San Diego, La Jolla CA 92093

[2]Cold Spring Harbor Laboratory, Cold Spring Harbor NY 11724

[3]Brookhaven National Laboratory, Upton, NY 11973

Abstract

The cellular basis of depressive disorders is poorly understood1. Recent studies in monkeys indicate that neurons in the lateral habenula (LHb), a nucleus that mediates communication between forebrain and midbrain structures, can increase their activity when an animal fails to receive an expected positive reward or receives a stimulus that predicts aversive conditions (i.e. disappointment or anticipation of a negative outcome)2, 3, 4. LHb neurons project to and modulate dopamine-rich regions such as the ventral-tegmental area (VTA)2, 5 that control reward-seeking behavior6 and participate in depressive disorders7. Here we show in two learned helplessness models of depression that excitatory synapses onto LHb neurons projecting to the VTA are potentiated. Synaptic potentiation correlates with an animal's helplessness behavior and is due to an enhanced presynaptic release probability. Depleting transmitter release by repeated electrical stimulation of LHb afferents, using a protocol that can be effective on depressed patients8, 9, dramatically suppresses synaptic drive onto VTA-projecting LHb neurons in brain slices and can significantly reduce learned helplessness behavior in rats. Our results indicate that increased presynaptic action onto LHb neurons contributes to the rodent learned helplessness model of depression.

To study the cellular basis of behavioral depression we examined the synaptic circuitry in the LHb of rats displaying learned helplessness (LH), a model of depression whereby

---

[#]Correspondence: Roberto Malinow, MD PhD, 9500 Gilman Drive # 0634, La Jolla CA 92093, rmalinow@ucsd.edu, Bo Li, PhD, 1 Bungtown Road, Cold Spring Harbor NY 11724, bli@cshl.edu.

[*]these authors contributed equally to this work

Supplementary Information is linked to the online version of the paper at www.nature.com/nature.

Author Contributions

B.L., J.P., M.M., and C.C contributed equally to the study; B.L., J.P., M.M., C.C., C.D.P. and D.S. performed and analyzed experiments; C.C. and B.L. made the figures; B.L., F.H. and R.M. designed the study; B.L. and R.M. wrote the manuscript.

Author Information

Reprints and permissions information is available at www.nature.com/reprints. The authors declare no competing financial interests. Readers are welcome to comment on the online version of this article at www.nature.com/nature.

animals show reduced escape from escapable foot shock10. We employed two well-established animal models: acute learned helplessness (aLH), which is induced by subjecting rats to periods of inescapable and unpredictable shock (aLH)10; and congenital learned helplessness (cLH), a strain of rats produced by selective breeding of animals displaying the greatest amount of aLH11, 12. In addition to showing reduced escape from escapable footshock, cLH and aLH animals also showed increased immobility in the forced swim test, another widely used animal model for depression13, compared with control animals (Fig. 2 a, b).

We examined transmission onto LHb neurons, which receive major inputs from numerous brain regions involved in stress response (such as the entopeduncular nucleus, lateral hypothalamus, lateral preoptic area, medial prefrontal cortex, and the bed nucleus of the stria terminalis; Supp Fig. 1;14) and can control dopaminergic function in the midbrain4. We wished to determine if synaptic transmission onto LHb neurons is different in LH compared to normal animals. To record selectively from LHb neurons that can regulate dopamine neuron activity, we injected *in vivo* Alexa 488 conjugated Cholera toxin, a retrograde tracer, in the VTA. Two to three days later, we prepared brain slices that contained the LHb. A minority of neurons in the LHb displayed fluorescent cell bodies, which indicated their projection to the VTA (Supplemental Fig. 2 a & b). Notably, the LHb neurons that project to VTA and RMTg, a newly identified GABAergic relay station between LHb and VTA15, 16, form largely non-overlapping populations (Supplemental Fig. 2 c), indicating that we were able to selectively target LHb neurons directly projecting to the VTA. LHb neurons projecting to the VTA were glutamatergic, as indicated by their co-localization with the glutamate transporter EAAC1 and lack of GABAergic marker expression (Supplemental Fig. 3). We performed whole-cell patch clamp recordings on VTA-projecting neurons in acute parasagittal brain slices prepared from rats that were wild type control, aLH, cLH (naïve), or cLH rats exposed to mild stress (cLHms, see Behavioral Paradigms in Methods). We examined miniature excitatory postsynaptic currents (mEPSCs, in the presence of tetrodotoxin to block action potentials and picrotoxin to block GABA-A-mediated synaptic currents), which were mediated by AMPA-type glutamate receptors (Supplemental Fig. 4 a) and represent responses from individual synapses onto these cells. The mean frequency of mEPSCs recorded from VTA-projecting LHb neurons of aLH (3.7 ± 0.8, mean ± s.e.m., n=23), cLH (4.0±0.7, n=85) and cLHms (4.7 ± 0.7, n=70) rats was increased relative to WT controls (2.3 ± 0.2, n=82; $F(3,251) = 3.1$, $p < 0.03$, ANOVA; Fig. 1 a, b). In general, the distribution of mEPSC frequencies recorded across different cells in all groups displayed a bimodal distribution (Fig 1 c). Notably, the prevalence of neurons with high-frequency mEPSCs (>8 Hz; shaded region, Fig 1 b, c & d) was significantly higher in aLH (17%), cLH (14%) and cLHms (20%) compared to WT (2%; $p< 0.01$, c^2). To determine if the observed excitatory synaptic potentiation was quantitatively correlated to an animal's helpless behavior, we first tested animals (either WT or cLH) with an escape avoidance task, and subsequently prepared brain slices and recorded from VTA-projecting neurons. From each animal we recorded from at least five cells and plotted the average mEPSC frequency against the animal's helpless behavior (as measured by the fraction of trials the animal failed to escape from an escapable 10 sec foot shock; also see Fig. 2 b). The significant correlation (Fig. 2 c; $R^2= 0.69$, $F(1, 11)=24.85$, $p< 0.001$, $n = 13$ for all animals; $R^2=0.64$, $F(1,6)=10.7$,

p<0.05, n=8 for cLH animals only) indicates that the potentiation of excitatory transmission onto VTA-projecting LHb neurons is linked with an individual animal's helpless behavior. To examine the output of VTA-projecting neurons we measured their spontaneous action potentials, which were more frequent in cLH animals compared to WT controls (Fig. 2 d). We observed no differences among the various groups with respect to the amplitude of mEPSCs (Fig. 1 e), frequency or amplitude of miniature inhibitory postsynaptic currents (supplemental Fig 4 b, c). These results indicate that the excitatory synaptic input onto LHb neurons that project to the VTA is potentiated in the learned helplessness model.

The enhanced mEPSC frequency could be due to an increase in either the number of synapses, or the probability of presynaptic neurotransmitter release. To distinguish between these possibilities, we first measured the density of dendritic spines, sites of excitatory synapses, on the dendrites of VTA-projecting LHb neurons. There was no significant difference in spine density between the WT controls and cLH animals (Fig. 3 a), and there was also no obvious difference in the dendritic branching between the two groups (not shown), suggesting there was no major difference in the number of synapses between control and cLH animals.

To determine whether there is a change in the efficacy of presynaptic neurotransmitter release, we examined evoked transmission. Synaptic transmission onto LHb neurons (elicited by placing a stimulating electrode in the LHb) showed distinct properties: the evoked excitatory synaptic response had a very small NMDA receptor component (Supplemental Fig. 4 d) and the AMPA receptor component displayed strong inward rectification (Supplemental Fig. 4 e). To probe presynaptic function we evoked transmission with high frequency stimulation trains (10 stimuli delivered at 20 or 50 Hz). The decrease in the amplitude of EPSCs in response to successive pulses during a train of stimuli reflects presynaptic vesicle depletion; more depletion correlates with higher release probability17. VTA-projecting LHb neurons of cLH animals showed a faster (20 Hz: $F(9, 198)=2.32$, $p<0.05$; 50 Hz: $F(9, 198)=3.83$, $p<0.001$) and more extensive (20 Hz: $F(1, 22)=6.62$, $p<0.05$; 50 Hz: $F(1, 22)=7.15$, $p<0.05$; One-Way ANOVA with repeated measures) synaptic depression, compared with that in WT control animals (Fig. 3 b). Furthermore, with minimal stimulation, which is designed to activate few synapses (as indicated by the amplitude of non-failure responses that is similar to the mEPSC amplitude; Fig. 3 c), we measured synaptic transmission failure rate. Excitatory synaptic transmission onto VTA-projecting LHb neurons of cLH animals had a significantly lower failure rate compared with that of control animals (Fig. 3 c; n=7–9, $p<0.001$, bootstrap). These results indicate that the excitatory synaptic inputs onto VTA-projecting LHb neurons of helpless animals have a higher synaptic release probability; therefore repeated stimulation can deplete synaptic vesicles faster and more efficiently in helpless animals.

One treatment for clinical depression, currently under evaluation, is deep brain stimulation (DBS), consisting of continuously delivered high frequency electrical stimulation to various brain regions8, 18. In a recent clinical case, DBS of LHb produced a marked remission of treatment-resistant depression9. Notably, depression recurred when DBS was stopped (in two accidental episodes9). To examine the cellular effects of DBS, we recorded in brain slices synaptic transmission onto VTA-projecting LHb neurons evoked by placing a

stimulating electrode in the LHb. After a baseline period of evoked transmission, a DBS protocol used in patients (7 stimulus 130 Hz trains separated by 40 ms intervals) was continuously delivered through the same stimulation electrode; stimuli interleaved with the DBS trains permitted us to monitor evoked synaptic transmission (see details in methods). The DBS protocol produced a marked depression of excitatory synaptic transmission, which persisted for the DBS protocol period, and was reversed upon cessation of the DBS protocol (Fig. 4 a). Thus, a DBS protocol can effectively reduce excitatory synaptic transmission onto VTA-projecting LHb neurons.

We wished to test if reducing synaptic drive onto LHb neurons can modulate helpless behavior. Remarkably, the same DBS protocol as used in brain slices delivered to the LHb in aLH animals markedly ameliorated the helpless behavior as indicated by an increase in escape behavior (Fig. 4 b & c; Supplemental Fig. 5 a). This effect was dependent on both the intensity of stimulation, and the placement of the stimulation electrode: stimulating at 300 μA had a stronger behavioral effect and affected a larger volume within the LHb than stimulating at 150 μA (Fig. 4 b & c, and Supplemental Fig. 5 b & c); and only if the electrode was placed in the lateral habenula, but not in the nearby thalamus, did DBS reverse the helplessness (Fig. 4 b, c, & e). Furthermore, DBS in LHb, but not sham stimulation in LHb, prevented the increase in immobility in the forced swim test (Fig. 4 d). Thus, suppression of synaptic transmission at the LHb through DBS can acutely reverse helpless behavior in rats.

A number of changes in neural function have been identified in depressed humans and rodent models of depression, likely due to the multifaceted nature of depressive disorders. 19, 20, 21, 22, 23 The recent identification of the LHb as a brain region in monkeys that can encode disappointment and expectation of negative conditions2, 3 led us to investigate its role in the learned helplessness rodent model of depression. Our findings indicate that excitatory synaptic activity onto VTA-projecting neurons in the LHb may be a key modulator of learned helplessness. The two learned helplessness models examined showed potentiated excitatory synaptic activity onto these neurons. Interestingly, the major modification was an increase in the proportion of cells displaying high-frequency mEPSCs in LH animals, from 2% to 14–20%. This suggests that large changes in a small proportion of cells in the LHb may be capable of modifying behavior. A critical role for transmission onto LHb neurons is further supported by the strong correlation between the potentiation of synaptic transmission onto VTA-projecting LHb neurons and an individual animal's helpless behavior. Given the presynaptic nature of synaptic potentiation, we examined the effects of synaptic depression by repeated afferent stimulation, a protocol that mimics clinically used DBS. Reducing synaptic transmission onto LHb neurons through a DBS protocol led to acute reversal of learned helplessness. Suppression of transmission onto VTA-projecting LHb neurons likely played a role in mediating this beneficial effect, although modulation of LHb neurons, or axons of passage, projecting to other targets may also be involved.

Our study provides cellular mechanisms that may explain previously reported phenomena: a) an increased LHb metabolic activity observed in depressed humans24, 25 and animal models of depression26, 27, and b) lesion28, 29 or pharmacological silencing30 of the LHb

can modulate depression-like symptoms in animal models. Our findings suggest an aberrant cellular process previously unexamined in the context of mood disorders that may be critical in the etiology of depression. Future studies aimed at determining the molecular signaling changes underlying the synaptic hyperactivity onto LHb neurons may lead to novel and effective treatments potentially able to reverse some forms of depressive disorders.

Methods Summary

Standard surgical procedures were followed for the *in vivo* injection of retrograde tracers. The cLH rats were bred as described11, 12. To prepare aLH animals, the rats were exposed to a LH "training session" after *in vivo* injection of retrograde tracers into VTA. This session consisted of inescapable, uncontrollable electric foot-shocks, with random shock duration and unpredictable inter-shock intervals. Control animals were placed in the shocking chamber in parallel without shocking. To prepare cLH animals exposed to mild stress (the cLHms group), cLH rats were treated with brief, escapable foot shock. Acute brain slices were prepared from different groups for electrophysiological recordings. To evaluate LH behavior, we employed both a lever pressing and an active avoidance task. In the lever pressing task a lever was added to the shocking chamber in the testing session. Foot shook was terminated if the animal pressed the lever. The active avoidance task was performed in a shuttle box equipped with an electrical grid floor and a door separating the two halves. Foot shock was terminated if the animal crossed to the other side of the cage. For the FST, the animal was forced to swim in a cylinder of water at 25 – 26 °C, and animal's immobility in the water was measured. To test the effect of DBS on LH behavior, rats were first trained and tested, and those that met the LH criteria were chosen for electrode implantation in LHb. After recovery from surgery rats underwent a training session followed by a 'baseline' LH test. DBS at different intensities was subsequently applied, and animals were tested again for the LH behavior. To test the effects of DBS on the FST, DBS in LHb was applied prior to the second day swimming to determine its effect on animal's immobility.

Methods

Animals

Wild-type male Sprague-Dawley rats were purchased from Taconic Farms and allowed to acclimate to the animal facility for 1 to 2 weeks prior to experiments. The cLH rats were bred as described11, 12. The rats were housed under a 12–12 hour light-dark cycle (7am–7pm), with food and water freely available. All procedures involving animals were approved by the Institute Animal Care and Use Committees of Cold Spring Harbor Laboratory, University of California, San Diego, and Brookhaven National Laboratory.

Retrograde labeling of VTA-projecting LHb neurons in vivo

Standard surgical procedures were followed for the *in vivo* injection31. To label the VTA-projecting LHb neurons we injected *in vivo* Alexa 488 conjugated Cholera toxin (2 μg/μl; Molecular Probes) or a herpes simplex virus expressing EGFP (HSV-GFP; NeuroVex, Oxon, UK), both of which are retrograde tracers, into the VTA.

Animals were anaesthetized with isoflurane (Baxter) using an isoflurane Vaporizer (Paragon Medical) and positioned in a stereotaxic apparatus that is connected to a computer system with a digital rat brain atlas (Angle Two Stereotaxic System, myNeuroLab.com). Injections of tracer solutions (3–5 injection sites along the vertical axis; 100–200 nl per injection) were delivered with a glass micropipette through a skull window (2–3 mm^2) by pressure application (5–12 psi, controlled by a Picrospritzer II, General Valve, Fairfield, NJ, USA). The injections were performed within the following stereotaxic coordinates: −5.3 mm from Bregma; 0.96 mm lateral from midline, and 8 to 8.4 mm vertical from cortical surface. Rats were injected subcutaneously with 5 mg/kg carprofen (NSAID) after surgery. During procedures, animals were kept on a heating pad and were brought back into their home cages after regaining movement. We waited 2 to 3 days to allow the retrograde labeling of neurons in the LHb before we sacrificed the animals for experiments.

Preparation of acute brain slices and electrophysiology

Male, 40 to 50-days-old rats were used for all the electrophysiology experiments. Animals were anesthetized with isoflurane, decapitated and the brains quickly removed and chilled in ice-cold dissection buffer (110.0 mM choline chloride, 25.0 mM NaHCO3, 1.25 mM NaH2PO4, 2.5 mM KCl, 0.5 mM CaCl2, 7.0 mM MgCl2, 25.0 mM glucose, 11.6 mM ascorbic acid, 3.1 mM pyruvic acid; gassed with 95%O2/5%CO2). Sagital slices (400 μm) across the LHb are cut in dissection buffer using a VT-1000 S vibratome (Leica, Nussloch, Germany) and subsequently transferred to a storage chamber containing artifical cerebrospinal fluid (ACSF; 118 mM NaCl, 2.5 mM KCl, 26.2 mM NaHCO3, 1 mM NaH2PO4, 20 mM Glucose, 4 mM MgCl2, 4 mM CaCl2; 22°–25°C; pH 7.4; gassed with 95%O2/5%CO2). After at least 1hr of recovery time slices are transferred to the recording chamber and are constantly perfused with ACSF maintained at 27°C.

Experiments were always performed on interleaved control and cLH or aLH animals. About 3/4 of the experiments were done blind to experimental group, which showed the same results as the non-blind data and were combined. Whole-cell patch clamp recordings were obtained with Axopatch-1D amplifiers (Axon Instruments) onto neurons in the LHb under visual guidance using transmitted light illumination. For evoked EPSC, synaptic transmission was evoked with a bipolar stimulating electrode placed close to the stria medullaris, typically > 0.2 mm away from cell bodies. Responses were recorded at holding potentials of −60 mV (for AMPA receptor-mediated responses) and +40 mV (for detection of any NMDA receptor-mediated responses and measurement of rectification). NMDA receptor-mediated responses were quantified as the mean current between 110 and 160 ms after stimulation. Bathing solution (ACSF) contained: (in mM): 119 NaCl, 2.5 KCl, 2 $CaCl_2$, 1 $MgCl_2$, 26.2 $NaHCO_3$, 1 NaH_2PO_4, 11 glucose, 0.1 picrotoxin and gassed with 5 % CO_2 and 95% O_2 at 27 °C (unless otherwise noted). Internal solution for voltage-clamp experiments contained: (in mM): 115 cesium methanesulfonate, 20 CsCl, 10 HEPES, 2.5 $MgCl_2$, 4 Na_2-ATP, 0.4 Na-GTP, 10 Na-phosphocreatine, and 0.6 EGTA (pH 7.2). Spermine (100 μM) was included in the internal solution for measurement of rectification. Miniature excitatory postsynaptic currents (mESPCs) were recorded at 27°C in the presence of 1 μM TTX and 100 mM picrotoxin in sagittal slices and analyzed using Mini Analysis

Program (Synaptosoft). To isolate miniature inhibitory spontaneous responses (mIPSCs), 1 μM TTX, 100 μM APV and 3 μM NBQX were added.

For the experiments in which high frequency stimulation trains were used to determine presynaptic release probability, QX314 (5 mM) was included in the internal solution to prevent the generation of sodium spikes. In order to recruit maximal number of axon terminals that can be stimulated by the high frequency trains, thereby minimizing the effects of axonal failures and reducing the variability in responses, low concentration (100 nM) of NBQX was included in the bath ACSF. This allows the stimulation at a higher intensity without evoking large EPSCs that could activate voltage-dependent conductances. For experiments testing the effects of DBS on synaptic transmission onto VTA-projecting LHb neurons, evoked EPSCs were monitored before, during, and after a stimulation protocol mimicking clinical DBS. Stimulation consisted of episodes of 44 trains of stimuli separated by 40 msec. During each train 7 stimuli were applied at a frequency of about 130 Hz. The inter-episode interval was 200 msec, during which two stimuli separated by 50 msec were applied to monitor the amplitude and slope of the EPSP. The DBS protocol and the paired-pulse stimulation were delivered using the same electrode.

Two-photon imaging of dendritic spines

Image acquisition and analysis were described previously32, 33. Images were acquired on a custom built dual channel 2-photon laser-scanning microscope (based on Olympus Fluoview laser-scanning microscope) using a Ti:Sapphire Chameleon laser (Coherent, Kitchener, Ontario, Canada) mode-locked to 910 nm. Full three-dimensional (3D) image stacks were acquired using a 60x 0.9 NA objective lens at 5x digital zoom (Fluoview software; Olympus), 70 nm per pixel. Each image plane was resampled three times and spaced 0.5 μm in the Z-dimension.

Behavioral Paradigms

Methods for the LH paradigm have been optimized previously34. To prepare learned helplessness animals (the aLH group) for behavioral testing and electrophysiological recording, the rats were exposed to a LH “training session” 5 days after *in vivo* injection of retrograde tracers into VTA. This session consisted of 120 inescapable, uncontrollable electric foot-shocks at 0.8 mA over 40 min in the shocking chambers (Coulbourn Instruments, PA; the chambers were 12"Wx10"Dx12"H and were controlled by Precision adjustable shockers), with random shock duration ranging from 5–15 seconds, and unpredictable inter-shock intervals (ITI’s). Experiments were performed on pairs of littermates housed in the same cage. Control animals were placed in the shocking chamber in parallel for 40 minutes without shocking. Electrophysiological recordings on acute brain slices were performed 24 to 48 hours after shocking. Animal identity was coded for blinding the researcher with respect to treatment. To prepare cLH animals exposed to mild stress (the cLHms group), cLH rats were treated with a procedure essentially the same as the active avoidance task (see below), during which animals received an average of 152± 27 seconds of escapable foot shock (n=8) and acute brain slices were prepared after 2 hours.

To evaluate LH behavior, we employed both a lever pressing task and an active avoidance task. The lever pressing task was described previously34. Briefly, an illuminated lever was added to the shocking chamber in the testing session, which was comprised of 15 escapable foot-shocks lasting up to 60 s (shorter if terminated by a lever press) over 21 min, and with fixed ITI's of 24 seconds. The active avoidance task was performed in a shuttle box (20"Wx10"Dx12"H; Coulbourne Instrument, PA) equipped with an electrical grid floor, a door separating the two halves, and photocell detectors. Shuttle box was placed in a sound attenuating chamber to minimize external stimuli. Testing was fully automated using Graphic State software (Coulbourne Instrument, PA). Animals were allowed to explore the shuttle box for 5 min and helpless behavior was evaluated over 30 trials of unexpected and escapable foot shock (1.2 mA intensity, 10 seconds duration, with random ITI's of 24 ± 12 s) following 5 s cue tone. Foot shock was terminated if the animal completely crossed to the other side of the cage. When an animal crossed the cage during the 5 s cue tone presentation, avoidance was scored. If an animal crossed during the 10 s shocks, the mean escape latency was measured. Failure was recorded if no crossing was made during the 10 s shock.

For the forced swim test, animals were forced to swim for 5 minutes in a cylinder of water (water temperature was 25 – 26 °C; the cylinder was 30 cm in diameter and 40 cm height; the depth of the water set to prevent animals from touching the bottom with their hind limbs). Animal behavior was videotaped using a PC6EX3 IR camera (Super Circuits). The immobile time each animal spent during the test was manually counted offline, with the evaluator being blind to the treatment of the animals.

Deep Brain Stimulation (DBS)

To prepare LH animals for the DBS experiments, animals were first treated with a 'training' session and 24 hours later a 'testing' session as described above. Based on the test results, animals that met the criteria (those pressed the lever only 0–5 times, and took between 16–21 min to finish the test) were used to test the effects of DBS. For increased stringency, only lever presses occurring within the first 20 seconds of shock onset were counted. 52 male Sprague Dawley rats were trained and tested, and 26 animals tested met the criteria. Three days later, standard surgical procedures were employed to implant bipolar concentric electrodes (8 mm in length, 0.8 mm tip Ø; Plastics One) unilaterally into the LHb (coordinates [mm]: −3.7 AP, ±0.7 ML, −5.4 DV) in rats that met the criteria.

After 3–5 days of recovery from surgery rats underwent a training session followed by a 'baseline' LH test. 3 animals, in which the electrodes were implanted into the LHb, were excluded from further study because their performance did not meet the criteria during the baseline test. Immediately following the baseline test, DBS (7 stimulus 130 Hz trains separated by 40 ms intervals; 150 μA intensity) in LHb, thalamus, or no stimulation (Sham) was applied for one hour. 24 hours later, another one-hour session of DBS or Sham stimulation was given immediately prior to and during the LH test. DBS intensity was 150 μA. Another 24 hours later, the final one-hour session of DBS or Sham stimulation was given at a higher intensity (300 μA), immediately prior to and during the final LH test (see Fig. 4 b for a schematic diagram showing the experimental procedures). Only animals with

electrode correctly placed in the LHb or thalamus (LPLR) were included for the respective behavioral analysis.

To test the effects of DBS on FST, electrodes were implanted in the same way as described above, except that in the DBS group, 2 rats had bilateral implants, and that in the Sham group 3 rats had bilateral implants. The rest of the animals had unilateral implants (total animals used for FST: DBS n=9; Sham n=10). Immobility time was recorded during the first 5 min of a 15-min swimming session on day 1. DBS (150 μA) or Sham stimulation was applied for 1 hour following FST on day 1. 24 hrs later (day 2), another 1 hour of DBS (150 μA) or Sham stimulation was applied and immobility time was recorded during the 5-min swimming session.

To determine the volume of tissue affected by DBS in LHb, in a separate set of experiments, animals were perfused with 4% PFA 2 hrs after the onset of DBS and brains were processed for immunohistochemistry to examine c-Fos expression.

Immunohistochemistry

Immunohistochemistry experiments were performed following standard procedures on 50 μm brain sections fixed with 4% PFA. The antibodies used were: anti-NeuN antibody (Chemicon, Temacula, CA); anti-EAAC1 antibody (Chemicon, Temacula, CA); anti-GABA antibody (Sigma); anti-GAD67 antibody (Chemicon, Temacula, CA); anti-c-Fos antibody (Santa Cruz biotechnology, Santa Cruz, CA). After finishing the immunohistochemistry process images were taken using either a Zeiss LSM 510 confocal microscope (for double labeling with two colors) or an Olympus BX41 histology microscope (for single labeling with one color), using 20X objectives.

Statistics and Data Presentation

To compare the means of non-normally distributed data sets we used a bootstrap procedure. Two data sets (N and M of size n and m) were randomly sampled n and m times, respectively (allowing resampling), and means (N_i and M_i) were generated. This procedure was repeated 10000 times. If N_j was more than M_j fewer than 5 % of the times, then the probability that N is more than M was estimated to be less than 0.05. Similar calculations established probabilities less than 0.01. All other statistical tests are indicated when used. All data are presented as mean ± s.e.m.

Supplementary Material

Refer to Web version on PubMed Central for supplementary material.

Acknowledgements

We thank Dr. Karl Deisseroth for help and suggestions, Andrew Gifford and Anat Biegon for sharing equipment and laboratory space, and members of the Malinow Lab and Li Lab for helpful discussions. B.L. is supported by the Dana Foundation and the Biobehavioral Research Awards for Innovative New Scientists (BRAINS) from NIH/NIMH (1R01MH091903-01). R.M. is supported by the Shiley-Marcos endowment.

References

1. Krishnan V, Nestler EJ. The molecular neurobiology of depression. Nature. 2008; 455(7215):894. [PubMed: 18923511]
2. Matsumoto M, Hikosaka O. Lateral habenula as a source of negative reward signals in dopamine neurons. Nature. 2007; 447(7148):1111. [PubMed: 17522629]
3. Matsumoto M, Hikosaka O. Representation of negative motivational value in the primate lateral habenula. Nat Neurosci. 2009; 12(1):77. [PubMed: 19043410]
4. Hikosaka O. The habenula: from stress evasion to value-based decision-making. Nat Rev Neurosci. 11(7):503. [PubMed: 20559337]
5. Ji H, Shepard PD. Lateral habenula stimulation inhibits rat midbrain dopamine neurons through a GABA(A) receptor-mediated mechanism. J Neurosci. 2007; 27(26):6923. [PubMed: 17596440]
6. Nestler EJ, Carlezon WA Jr. The mesolimbic dopamine reward circuit in depression. Biol Psychiatry. 2006; 59(12):1151. [PubMed: 16566899]
7. Krishnan V, et al. Molecular adaptations underlying susceptibility and resistance to social defeat in brain reward regions. Cell. 2007; 131(2):391. [PubMed: 17956738]
8. Mayberg HS. Targeted electrode-based modulation of neural circuits for depression. J Clin Invest. 2009; 119(4):717. [PubMed: 19339763]
9. Sartorius A, et al. Remission of major depression under deep brain stimulation of the lateral habenula in a therapy-refractory patient. Biol Psychiatry. 67(2):e9. [PubMed: 19846068]
10. Maier SF. Learned helplessness and animal models of depression. Prog Neuropsychopharmacol Biol Psychiatry. 1984; 8(3):435. [PubMed: 6385140]
11. Henn FA, Vollmayr B. Stress models of depression: forming genetically vulnerable strains. Neurosci Biobehav Rev. 2005; 29(4–5):799. [PubMed: 15925700]
12. Schulz D, Mirrione MM, Henn FA. Cognitive aspects of congenital learned helplessness and its reversal by the monoamine oxidase (MAO)-B inhibitor deprenyl. Neurobiol Learn Mem. 2010; 93(2):291. [PubMed: 19931627]
13. Porsolt RD, Le Pichon M, Jalfre M. Depression: a new animal model sensitive to antidepressant treatments. Nature. 1977; 266(5604):730. [PubMed: 559941]
14. Lecourtier L, Kelly PH. A conductor hidden in the orchestra? Role of the habenular complex in monoamine transmission and cognition. Neurosci Biobehav Rev. 2007; 31(5):658. [PubMed: 17379307]
15. Jhou TC, et al. The rostromedial tegmental nucleus (RMTg), a GABAergic afferent to midbrain dopamine neurons, encodes aversive stimuli and inhibits motor responses. Neuron. 2009; 61(5): 786. [PubMed: 19285474]
16. Kaufling J, et al. Afferents to the GABAergic tail of the ventral tegmental area in the rat. J Comp Neurol. 2009; 513(6):597. [PubMed: 19235223]
17. Zucker RS, Regehr WG. Short-term synaptic plasticity. Annu Rev Physiol. 2002; 64:355. [PubMed: 11826273]
18. Sartorius A, Henn FA. Deep brain stimulation of the lateral habenula in treatment resistant major depression. Med Hypotheses. 2007; 69(6):1305. [PubMed: 17498883]
19. Airan RD, et al. High-speed imaging reveals neurophysiological links to behavior in an animal model of depression. Science. 2007; 317(5839):819. [PubMed: 17615305]
20. Berton O, Nestler EJ. New approaches to antidepressant drug discovery: beyond monoamines. Nat Rev Neurosci. 2006; 7(2):137. [PubMed: 16429123]
21. Pittenger C, Duman RS. Stress, depression, and neuroplasticity: a convergence of mechanisms. Neuropsychopharmacology. 2008; 33(1):88. [PubMed: 17851537]
22. Sahay A, Hen R. Adult hippocampal neurogenesis in depression. Nat Neurosci. 2007; 10(9):1110. [PubMed: 17726477]
23. Mill J, Petronis A. Molecular studies of major depressive disorder: the epigenetic perspective. Mol Psychiatry. 2007; 12(9):799. [PubMed: 17420765]
24. Morris JS, et al. Covariation of activity in habenula and dorsal raphe nuclei following tryptophan depletion. Neuroimage. 1999; 10(2):163. [PubMed: 10417248]

25. Roiser JP, et al. The Effects of Tryptophan Depletion on Neural Responses to Emotional Words in Remitted Depression. Biol Psychiatry. 2009
26. Shumake J, Gonzalez-Lima F. Brain systems underlying susceptibility to helplessness and depression. Behav Cogn Neurosci Rev. 2003; 2(3):198. [PubMed: 15006293]
27. Caldecott-Hazard S, Mazziotta J, Phelps M. Cerebral correlates of depressed behavior in rats, visualized using 14C-2-deoxyglucose autoradiography. J Neurosci. 1988; 8(6):1951. [PubMed: 3385484]
28. Amat J, et al. The role of the habenular complex in the elevation of dorsal raphe nucleus serotonin and the changes in the behavioral responses produced by uncontrollable stress. Brain Res. 2001; 917(1):118. [PubMed: 11602236]
29. Yang LM, et al. Lateral habenula lesions improve the behavioral response in depressed rats via increasing the serotonin level in dorsal raphe nucleus. Behav Brain Res. 2008; 188(1):84. [PubMed: 18054396]
30. Winter C, et al. Pharmacological inhibition of the lateral habenula improves depressive-like behavior in an animal model of treatment resistant depression. Behav Brain Res. 2011; 216(1):463. [PubMed: 20678526]
31. Rumpel S, LeDoux J, Zador A, Malinow R. Postsynaptic receptor trafficking underlying a form of associative learning. Science. 2005; 308(5718):83. [PubMed: 15746389]
32. Kopec CD, et al. Glutamate receptor exocytosis and spine enlargement during chemically induced long-term potentiation. J Neurosci. 2006; 26(7):2000. [PubMed: 16481433]
33. Kopec CD, Real E, Kessels HW, Malinow R. GluR1 links structural and functional plasticity at excitatory synapses. J Neurosci. 2007; 27(50):13706. [PubMed: 18077682]
34. Vollmayr B, Henn FA. Learned helplessness in the rat: improvements in validity and reliability. Brain Res Brain Res Protoc. 2001; 8(1):1. [PubMed: 11522522]

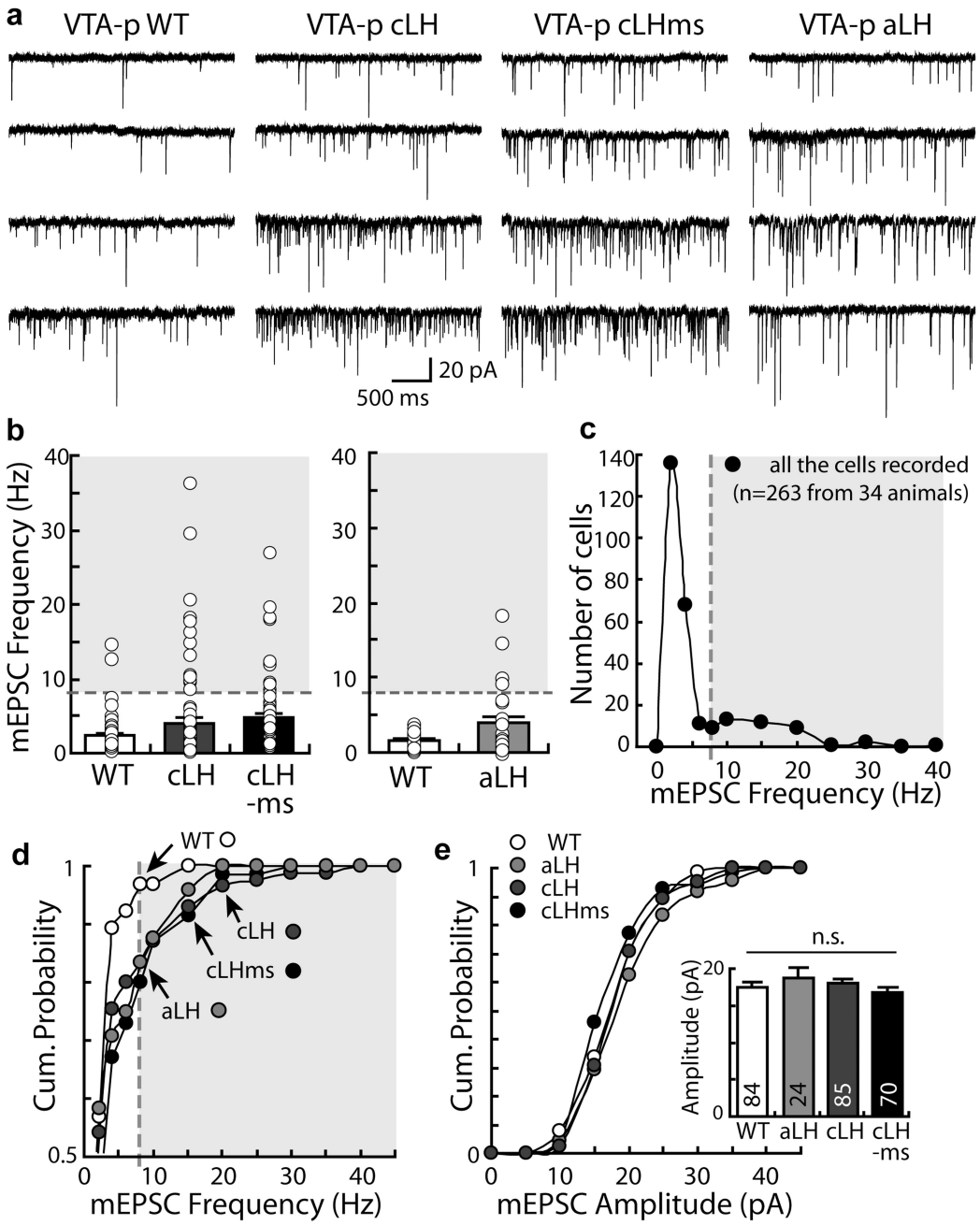

Figure 1. Increased excitatory synaptic transmission onto VTA-projecting LHb neurons in the learned helplessness models of depression

a. Examples of mEPSCs recorded from VTA-projecting LHb neurons (VTA-p) from WT, cLH, cLHms, and aLH animals. b. Means (bars) and individual recordings (circles) of mEPSC frequency from VTA-projecting LHb neurons in different groups of animals. Left, WT: 2.4±0.3, n=65 [6 animals]; cLH: 4.0±0.7, n=85 [8 animals], $p<0.05$, bootstrap; cLHms: 4.7±0.7, n=70 [8 animals], $p<0.001$, bootstrap). Right, WT: 1.8±0.2, n=19 [4 animals]; aLH: 3.9±1, n=24 [4 animals], $p<0.05$, bootstrap. c. Frequency distribution of mEPSC frequencies of all cells recorded exhibited bimodal distribution. d. The cumulative probability of mEPSC

frequency of VTA-projecting LHb neurons in different groups of animals ($p<0.05$, K-S test comparing WT with any other groups). e. The amplitude of mEPSC was not different among different animal groups ($p>0.3$, bootstrap). All error bars represent s.e.m.

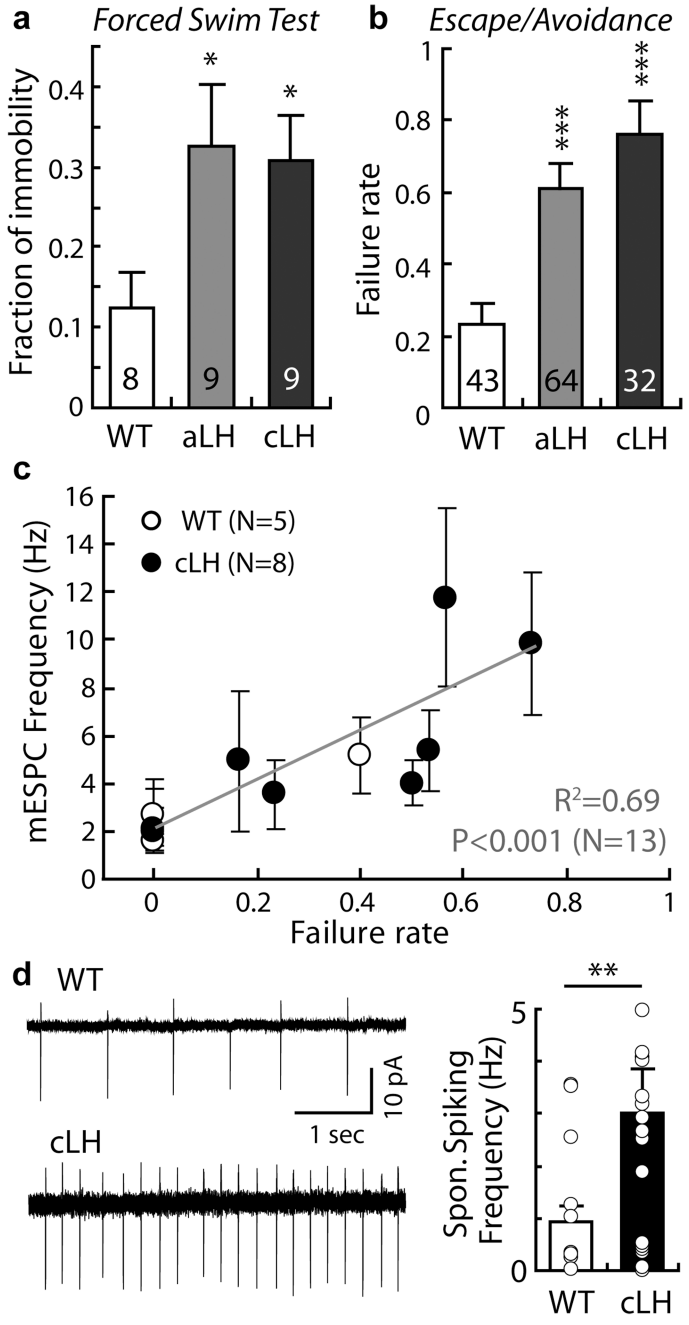

Figure 2. Enhanced synaptic transmission onto VTA-projecting LHb neurons correlates with helpless behavior of individual animals

a–b. aLH and cLH animals display behavioral deficits in the forced swim test (FST) and escape/avoidance test. a. Fraction of immobile time for 5 min in FST (WT: 0.12±0.05, aLH: 0.33±0.08, cLH: 0.31±0.05, n indicated in bars, *p<0.05, Kruskal-Wallis test). b. Failure rate to escape during 30 trials of escapable footshock (WT: 0.12±0.03, aLH: 0.31±0.03, cLH: 0.38±0.05, n indicated in bars, ***p<0.001, F(2, 136)=11.57, one way ANOVA). c. Mean mESPC frequency onto VTA-projecting LHb neurons correlates with an animal's helpless behavior measured as the fraction of sessions in which animals failed to escape

(R^2=0.69; p< 0.001, N=13 animals, n>5 cells for each animal). d. Spontaneous spiking rate measured in cell attached configuration was increased in cLH compared to WT control animals (WT: 0.92±0.32, cLH: 3.03±0.82, n=17–25, **p<0.01, bootstrap). All error bars represent s.e.m.

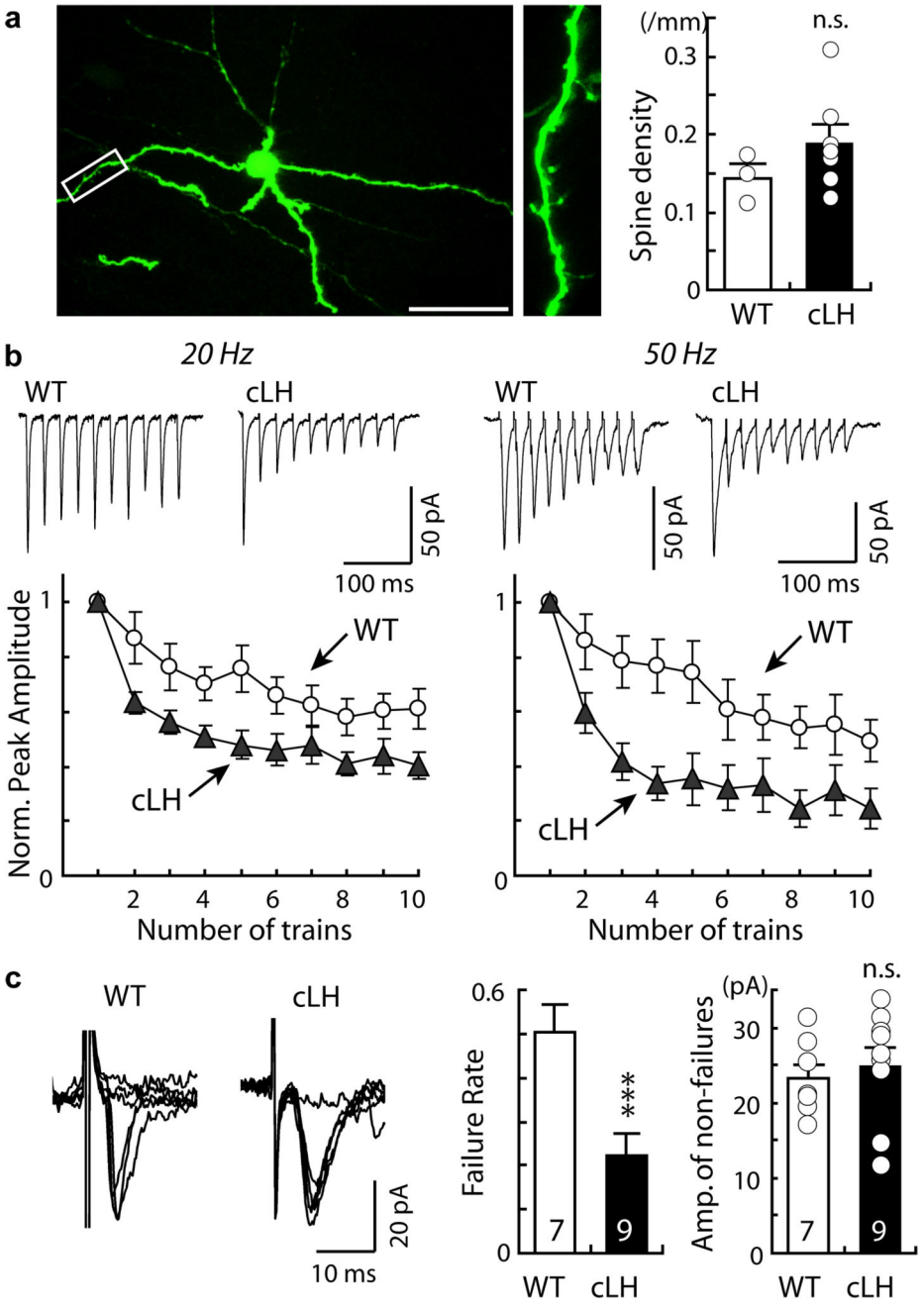

Figure 3. Presynaptic mechanism underlying the increase in excitatory synaptic transmission onto VTA-projecting LHb neurons in helpless animals

a. Two-photon laser scanning images of a VTA-projecting LHb neuron labeled by *in vivo* injection into the VTA of a retrogradely transported HSV-GFP virus in low (left) and high (middle) magnifications. Scale bar: 50 μm. Right, dendritic spine density on VTA-projecting LHb neurons of WT or cLH animals (WT: 0.15±0.02, 3 cells, 1125.3 μm total dendritic length; cLH: 0.18±0.02, 7 cells, 1002.4 μm total dendritic length; p>0.1, t-test). b. Top, evoked EPSCs onto VTA-projecting LHb neurons of WT or cLH animals in response to stimulus trains (20 Hz or 50 Hz). Bottom, plot of peak EPSCs normalized to first EPSC

(WT: 20 Hz n=10, 50 Hz n=11; cLH: 20 Hz n=14, 50 Hz n=13). Compare to WT, cLH animals showed a faster (20 Hz: $F(9, 198)=2.32$, $p=0.02$; 50 Hz: $F(9, 198)=3.83$, $p<0.001$) and more extensive (20 Hz: $F(1, 22)=6.62$, $p=0.02$; 50 Hz: $F(1, 22)=7.15$, $p=0.01$; One-Way ANOVA with repeated measures). c. Left, minimally evoked EPSCs onto VTA-projecting LHb neurons (left) display more failures (middle) in WT than cLH animals (WT: 0.5±0.1, n=7; cLH: 0.2±0.1, n=9, ***$p<0.001$, t-test). Right, mean amplitude of successful trials (WT: 23.2 ±2 pA, n=7; cLH: 24.8±2.5 pA, n=9; $p>0.6$, t-test). All error bars represent s.e.m.

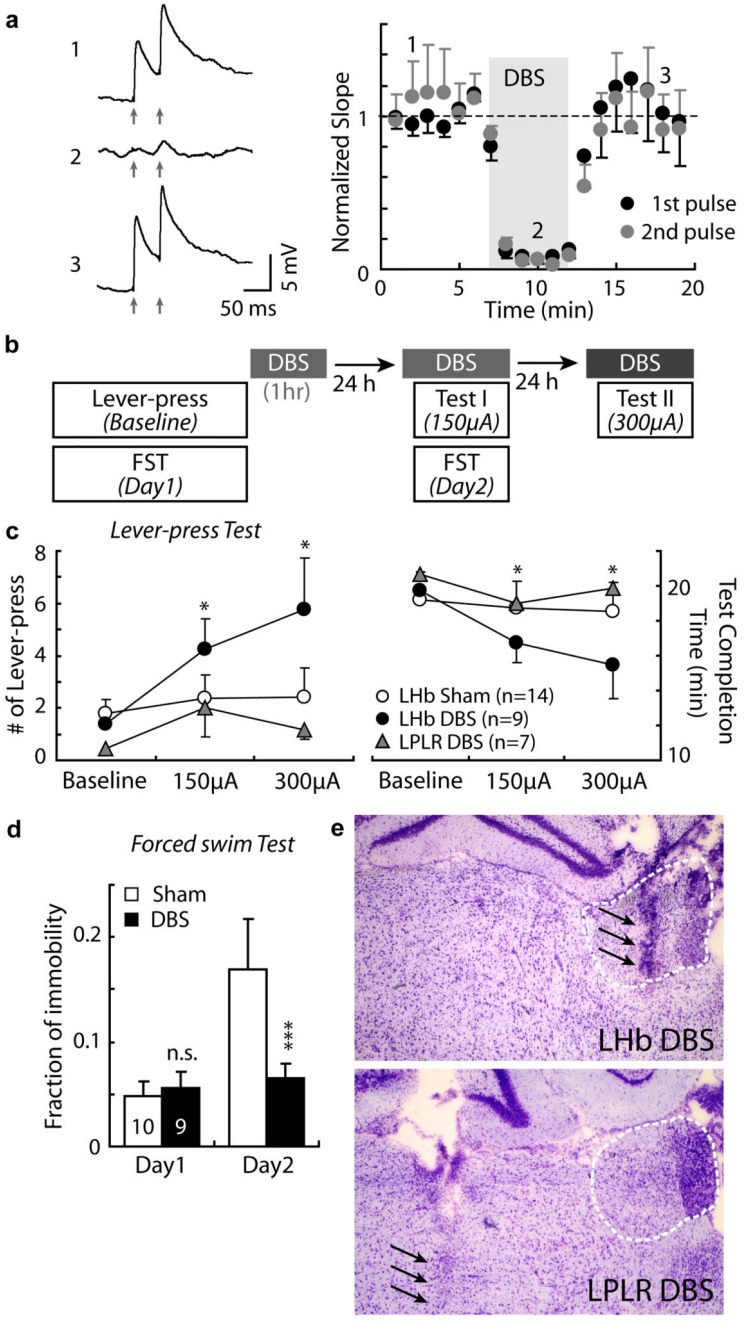

Figure 4. DBS in LHb suppresses excitatory synaptic transmission and reverses learned helplessness

a. Left, example EPSPs (paired-pulses) recorded from a VTA-projecting LHb neuron before (1), during (2), and after (3) stimulation mimicking DBS. Arrows indicate when paired-pulses were given. Right, average EPSP slope at indicated time points: 1) before (first pulse 1.1±0.1; second pulse 0.9±0.1; n=6, [4 animals]); 2) during (first pulse 0.2±0.07; second pulse 0.03±0.03), $p < 0.001$ for both pulses compared with those in 1); and 3) after (first pulse 1.2±0.3; second pulse 0.9±0.2) DBS. b. A schematic diagram showing the experimental procedures. c. Lever presses (left) and test completion time (right) for animals

received DBS or sham stimulation in the LHb, or DBS in the LPLR (lateral post thalamic nuclei, laterorostral), before (baseline) or after DBS of different intensities. DBS in LHb (n=9): Lever press baseline 1.2±0.4; 150 μA session 3.9±1; 300 μA session (n=8) 5.8±2. Test completion time baseline 19.9±0.4; 150 μA session 17.1±1; 300 μA session (n=8) 15.4±2. Sham (n=14): Lever press baseline 1.8±0.5; 150 μA session 2.4±0.9; 300 μA session 2.4±1. Test completion time baseline 19.2±0.5; 150 μA session 18.7±0.9; 300 μA session 18.5±1.1. DBS in LPLR (n=7): Lever press baseline 0.4±0.2; 150 μA session 2±1; 300 μA session 1.1±0.3. Test completion time baseline 20.6±0.2; 150 μA session 19±1.2; 300 μA session 19.9±0.3. For DBS in LHb group, *$p < 0.05$ compared with baseline. Sham and DBS in LPLR group: $p > 0.05$ for both measurements at both sessions compared with baseline (bootstrap). d. Immobility during FST. DBS Day1: 0.06±0.01, Day2: 0.06±0.01, n = 9; Sham Day1: 0.05±0.01, Day2: 0.17±0.05, n = 10; DBS vs. Sham in Day2: *** $p < 0.001$, bootstrap. e. Representative cresyl violet staining of coronal brain sections; arrows indicate electrode track in the LHb (upper) or LPLR (lower). All error bars represent s.e.m.